

The Bulk Photovoltaic Effect: Origin of Shift Currents in the Many-Body Picture

MingRui Lai,^{1,2} Fengyuan Xuan,^{3,2} and Su Ying Quek^{3,2,1,4,*}

¹*Integrative Sciences and Engineering Programme,
NUS Graduate School, National University of Singapore*

²*Centre for Advanced 2D Materials, National University of Singapore, 6 Science Drive 2, Singapore 117546*

³*Department of Physics, National University of Singapore, 2 Science Drive 3, Singapore 117551*

⁴*Department of Materials Science and Engineering, National University of Singapore*

(Dated: October 10, 2024)

We show that the shift current in bulk photovoltaics originates from a light-induced shift of charge centers to the many-body excited states. This many-body shift vector is expressed, using a sum-rule, in terms of pairs of nearly-degenerate optically-active excitons overlapping in k -space. The shift current can thus be enhanced by nearly-degenerate optically-active and tightly-bound excitons, spread out in k -space. *Ab initio* results for the many-body shift current and shift vector are presented for CdS and MoS₂, and exciton-phonon coupling is included through the exciton-phonon self-energies.

The bulk photovoltaic effect (BPVE) is a strong contender for next-generation photovoltaic applications [1]. The BPVE stems from the static second-order optical response of a crystal with broken inversion symmetry and consists of the shift current, injection current, optical rectification [2], ballistic current [3] and recombination current [4]. For linearly polarized light at low temperatures, the shift current dominates the BPVE [5, 6]. The shift current is typically formulated within the independent particle approximation (IPA) where optical excitations are described by individual quasielectron and quasihole excitations. Early efforts in proposing designs of optimal materials for shift currents have relied on the IPA, even for low-dimensional materials [8].

It is known that photoexcitations in fact result in the formation of excitons—correlated electron-hole excitations—described using an effective two-body Bethe Salpeter Equation (BSE) approach [9]. In recent years, it has been found that two-dimensional (2D) layered materials [10, 11] can exhibit very large BPVE [12] and non-linear optical responses [13–15]; these 2D materials also offer the prospect of bottom-up design through integration with other materials [16, 17] or photonic devices [18, 19]. Due to reduced electronic screening in 2D [20], electron-hole interactions and hence excitonic effects are more pronounced. It therefore becomes increasingly important to establish an understanding of the shift current within the many-body formalism.

In this work, we derive an expression for the BPVE, considering the static current response of a crystal to linearly polarized light, from time-dependent perturbation theory, using as a basis the exciton states obtained from a first principles GW-BSE approach [9]. We treat the effects of exciton-phonon coupling by renormalizing the exciton energies using approximate exciton-phonon self-energies, but do not explicitly consider exciton-phonon scattering processes that might lead to ballistic currents. The resulting many-body expression for the BPVE reduces to the IPA expression in the non-interacting limit.

Our *ab initio* results for bulk CdS are in good agreement with experiment, demonstrating the role of excitons in the measured shift current. The many-body shift current expression leads to a natural definition of a many-body shift vector that is completely analogous with the IPA shift vector, when a sum rule is applied. The many-body shift vector, defined for each exciton, is a positional shift from the many-body ground state to the many-body excited state and is gauge-invariant.

We present a straight-forward approach to compute the many-body shift vector from first principles, and provide an alternative physical interpretation for the many-body shift vector in terms of matrix elements involving pairs of nearly-degenerate optically-active excitons that overlap in k -space. We thus demonstrate that the magnitude of the shift vector can be enhanced for nearly-degenerate excitons that are tightly bound in real space, and hence spread out in k -space. In the IPA limit, the excitons collapse to single v to c transitions at individual k -points, greatly reducing the likelihood of overlap in reciprocal space. First principles results for the MoS₂ monolayer show that the shift current conductivity is significantly enhanced by excitonic effects in this 2D material. This enhancement results not only from enhanced oscillator strength observed for a few low-energy peaks, but also from the fact that the magnitude of the shift vectors for most excitons are enhanced by an order of magnitude compared to their IPA counterparts.

The BPVE is defined as the second-order static current response to an incident electromagnetic field, using perturbation theory and taking the expectation value of the velocity operator. In the semi-classical approach where the electromagnetic field is defined as $E^\beta(t) = \frac{1}{\sqrt{2}}(E^\beta e^{i\omega t} + E^{\beta*} e^{-i\omega t}) e^{\eta t}$, the static current response can be partitioned, following Ref. [2], into the shift current, injection current, and optical rectification responses [24]. η is a small positive number to capture the adiabatic switching-on of the electromagnetic field. For linearly polarized light, we can define the shift current

conductivity $\sigma_{\beta\beta}^{\alpha,\text{shift}}$ as $j_{\alpha\beta\beta}^{(2),\text{shift}} = \sigma_{\beta\beta}^{\alpha,\text{shift}} |E^\beta|^2$. $\sigma_{\beta\beta}^{\alpha,\text{shift}}$ is derived (in the limit where $\eta \rightarrow 0^+$) to be

$$\begin{aligned} \sigma_{\beta\beta}^{\alpha,\text{shift}} &= \frac{-i\mathcal{C}}{\omega^2} \underbrace{\sum_{SS'} \frac{v_{0S'}^\alpha p_{S'S}^\beta p_{S0}^\beta}{\Omega_0 - \Omega_{S'}} \delta(\Omega_S - \Omega_0 - \omega)}_{\text{Term 1}} \\ &+ \frac{i\mathcal{C}}{\omega^2} \underbrace{\sum_{\Omega_S \neq \Omega_{S'}} \frac{v_{S'S}^\alpha p_{S0}^\beta p_{0S'}^\beta}{\Omega_{S'} - \Omega_S} \delta(\Omega_S - \Omega_0 - \omega) + (\omega \leftrightarrow -\omega)}_{\text{Term 2}}, \end{aligned} \quad (1)$$

where $\mathcal{C} = \frac{\pi e^3}{m^2 \hbar^2 v_{\text{cryst}}} < 0$. $|S\rangle$ is a many-body excited state and $|0\rangle$ is the many-body ground state. $\hbar\Omega_S$ is the exciton energy. We have suppressed the bra-ket notation (e.g. $\langle S' | \hat{v}^\alpha | S \rangle \equiv v_{S'S}^\alpha$, $\langle S' | \hat{p}^\alpha | S \rangle \equiv p_{S'S}^\alpha$). \hat{v} and \hat{p} are many-body operators with $\hat{v}^\alpha = \sum_i^N \hat{v}_{i,\text{sp}}^\alpha$ and $\hat{p}^\alpha = \sum_i^N \hat{p}_{i,\text{sp}}^\alpha$, where $\hat{v}_{i,\text{sp}}^\alpha$ and $\hat{p}_{i,\text{sp}}^\alpha$ are the single particle velocity and momentum operators. Our work is presented for cases where the light intensity is small enough for perturbation theory to be valid, but sufficiently large that the classical treatment of the electromagnetic field is valid - the case for most non-linear optical experiments [13, 25, 26]. Under these conditions, the recombination current, which does not depend on the incident light intensity, [4] is negligible compared to the shift current.

Using $[\hat{r}^\alpha, \hat{p}^\beta] = i\hbar\delta_{\alpha\beta}$, one can obtain a many-body sum rule [24] (see S2 for a derivation):

$$\sum_{S' \neq 0} r_{0S'}^\alpha p_{S'S}^\beta - \sum_{S' \neq S} p_{0S'}^\beta r_{S'S}^\alpha = R_{S0}^\alpha p_{0S}^\beta, \quad (2)$$

where

$$R_{S0}^\alpha = r_{S'S}^\alpha - r_{00}^\alpha. \quad (3)$$

Then $\sigma_{\beta\beta}^{\alpha,\text{shift}}$ becomes

$$\sigma_{\beta\beta}^{\alpha,\text{shift}} = \frac{\mathcal{C}}{\omega^2} \sum_S R_{S0}^\alpha |p_{0S}^\beta|^2 \delta(\Omega_S - \Omega_0 - \omega) + (\omega \leftrightarrow -\omega). \quad (4)$$

A comparison can be made to the IPA expression for the shift current conductivity: [2]

$$\sigma_{\beta\beta}^{\alpha,\text{IPA shift}} = \frac{\mathcal{C}}{\omega^2} \sum_{nm\mathbf{k}} \mathcal{R}_{nm\mathbf{k}}^\alpha |p_{nm\mathbf{k}}^\beta|^2 f_{nm\mathbf{k}} \delta(\omega_{m\mathbf{n}\mathbf{k}} - \omega), \quad (5)$$

where $\mathcal{R}_{nm\mathbf{k}}^\alpha = \frac{\partial \phi_{nm\mathbf{k}}}{\partial k^\alpha} + \xi_{nm\mathbf{k}}^\alpha - \xi_{m\mathbf{n}\mathbf{k}}^\alpha$ is defined as the IPA shift vector [2]. Here, $\xi_{nm\mathbf{k}}^\alpha = i \langle u_{n\mathbf{k}} | \frac{\partial u_{m\mathbf{k}}}{\partial k^\alpha} \rangle$ and ϕ_{nm} is the phase of the dipole matrix element. This comparison shows that the many-body shift vector can be analogously defined as R_{S0}^α , the positional shift from state $|0\rangle$ to state $|S\rangle$ (Eq. 3). A similar expression to Eq. 4 was recently obtained using the many-body theory of polarization. [27]

We construct the states $|S\rangle$ in the Tamm-Dancoff approximation with $|S\rangle = \sum_{v\mathbf{c}\mathbf{k}} A_{v\mathbf{c}\mathbf{k}}^S \hat{a}_{v\mathbf{c}\mathbf{k}}^\dagger \hat{a}_{v\mathbf{k}} |0\rangle$ [28] while the ground state $|0\rangle$ is constructed as a single Slater determinant of single particle states. $\hat{a}_{v\mathbf{k}}, \hat{a}_{v\mathbf{c}\mathbf{k}}^\dagger$ are the single particle annihilation and creation operators. The many-body excitation energies $E_S \equiv \hbar\Omega_S$ and $|S\rangle$ are obtained by solving the GW-BSE equation [9]:

$$(\varepsilon_{c\mathbf{k}} - \varepsilon_{v\mathbf{k}}) A_{v\mathbf{c}\mathbf{k}}^S + \sum_{v'\mathbf{c}'\mathbf{k}'} K_{v\mathbf{c}\mathbf{k},v'\mathbf{c}'\mathbf{k}'}^{eh} A_{v'\mathbf{c}'\mathbf{k}'}^S = E_S A_{v\mathbf{c}\mathbf{k}}^S \quad (6)$$

$\varepsilon_{n\mathbf{k}}$ are the quasiparticle energies calculated within the GW approximation [29] and $K_{v\mathbf{c}\mathbf{k},v'\mathbf{c}'\mathbf{k}'}^{eh}$ describes the electron-hole interactions. When electron-hole interactions are set to zero, $|S\rangle = \hat{a}_{v\mathbf{c}\mathbf{k}}^\dagger \hat{a}_{v\mathbf{k}} |0\rangle$, i.e., the ‘‘exciton’’ reduces to a transition from Bloch state $|v\mathbf{k}\rangle$ to $|c\mathbf{k}\rangle$. We can show analytically [24] (see section S3) that using this reduction, the many-body shift current conductivity and many-body shift vector reduce to their IPA counterparts. Fig. S1 illustrates this equivalence numerically for the shift current conductivity.

Using Blount’s formalism for the \hat{r} operator in terms of interband and intraband terms [30], we can also obtain

$$\begin{aligned} r_{S'S}^\alpha &= \underbrace{\sum_{\substack{v\mathbf{k} \\ c \neq c'}} A_{v\mathbf{c}\mathbf{k}}^{S'*} A_{v\mathbf{c}\mathbf{k}}^S \xi_{c\mathbf{k}}^\alpha - \sum_{\substack{c\mathbf{k} \\ v \neq v'}} A_{v\mathbf{c}\mathbf{k}}^{S'*} A_{v\mathbf{c}\mathbf{k}}^S \xi_{v\mathbf{k}}^\alpha}_{\text{Term a}} \\ &+ \underbrace{\sum_{v\mathbf{c}\mathbf{k}} A_{v\mathbf{c}\mathbf{k}}^{S'*} A_{v\mathbf{c}\mathbf{k}}^S (\xi_{c\mathbf{k}}^\alpha - \xi_{v\mathbf{k}}^\alpha) + i A_{v\mathbf{c}\mathbf{k}}^{S'*} \frac{\partial A_{v\mathbf{c}\mathbf{k}}^S}{\partial k_v^\alpha} - i A_{v\mathbf{c}\mathbf{k}}^S \frac{\partial A_{v\mathbf{c}\mathbf{k}}^{S'*}}{\partial k_c^\alpha}}_{\text{Term b}} \\ &+ r_{00}^\alpha \delta_{S'S}. \end{aligned} \quad (7)$$

For $S = S'$, Eq. 7 gives $R_{S0}^\alpha = r_{S'S}^\alpha - r_{00}^\alpha$ to be Terms a and b. The \mathbf{k} -derivatives in Term b ensure gauge invariance, similar to $\frac{\partial \phi_{nm}(\mathbf{k})}{\partial k^\alpha}$ in Eq. 5 (see S4) [24].

The expectation values of position for the many-body states, $r_{S'S}^\alpha$ and r_{00}^α , can be tricky to compute from first principles. However, Eq. 2 provides a straight-forward approach to compute the many-body shift vector for optically-active excitons. Specifically, the GW-BSE calculations give p_{0S}^β , and we also have

$$p_{S'S}^\beta = \sum_{v\mathbf{c}\mathbf{k}} A_{v\mathbf{c}\mathbf{k}}^{S'*} A_{v\mathbf{c}\mathbf{k}}^S p_{c'\mathbf{k}}^\beta - \sum_{v'\mathbf{c}\mathbf{k}} A_{v'\mathbf{c}\mathbf{k}}^{S'*} A_{v'\mathbf{c}\mathbf{k}}^S p_{v\mathbf{k}}^\beta. \quad (8)$$

We compute the position matrix elements using $p_{S'S}^\alpha / im(\Omega_{S'} - \Omega_S)$.

In Eq. 1, we assumed that the exciton energies were real-valued. When $|\Omega_{S'} - \Omega_S| \rightarrow 0^+$, Term 2 approaches infinity. In physical systems, excitons have finite lifetimes, which we include by adding to Ω_S the exciton-phonon self-energy Ξ_S , treated in the uncorrelated exciton approximation where $\Xi_S = \sum_{v\mathbf{c}\mathbf{k}} |A_{v\mathbf{c}\mathbf{k}}^S|^2 (\Sigma_{c\mathbf{k}} - \Sigma_{v\mathbf{k}}^*)$ [31] and $\Sigma_{n\mathbf{k}}$ are the electron-phonon self energies [32] for the Bloch state $|n\mathbf{k}\rangle$, computed from first

principles. This procedure results in complex quantities for $\sigma_{\beta\beta}^{\alpha, \text{shift}}$, and the real part is taken. Physically, only interexciton transitions that take place within the lifetimes of the excitons contribute to the shift current (see also S5) [24].

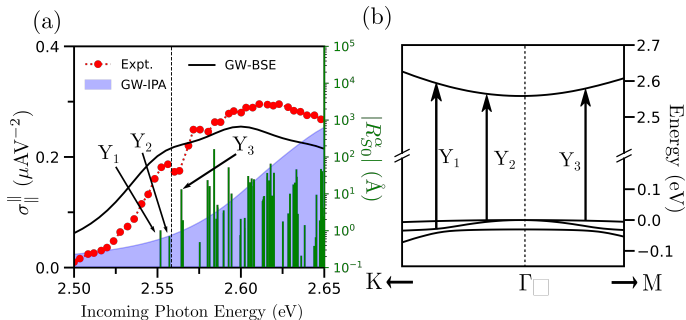


FIG. 1. (a) Shift current conductivity (left axis) and magnitude of the many-body shift vectors (right axis) for bulk CdS. The shift current conductivity is computed with GW-BSE (black curve) and GW-IPA (blue shaded region). Experimental data is taken from Ref. [33]. \parallel refers to the direction parallel to the polar axis. The vertical dashed line represents the quasiparticle band gap. A set of three nearly-degenerate excitons has been identified as Y_1 , Y_2 and Y_3 . (b) GW quasiparticle bandstructure around Γ for CdS, with vertical arrows indicating the interband transitions for the three excitons labelled in (a). The optical absorption spectra compared with experiment is shown in Fig. S2 and the IPA shift vectors in Fig. S3.

We apply our formalism to bulk CdS (Fig. 1(a)), and compare our results with the experimental shift current conductivity [33] measured at 2K, where ballistic currents are negligible. The many-body result is in better agreement with experiment [33] than the IPA. The crux of this result is that the experimentally observed below-gap shift current can only be accounted for using the many-body calculation. The magnitudes of the many-body shift vectors for optically active excitons are also shown in green in Fig. 1(a). The below-gap shift current conductivity is associated with shift vectors for the low-energy excitons, Y_1 and Y_2 . The nearly-degenerate excitons, Y_1 , Y_2 and Y_3 , originate from transitions near the Γ point, between the first three nearly-degenerate valence bands and the first conduction band (Fig. 1(b)). Examining Eq. 1 shows that we expect the many-body shift current to be dominated by contributions from nearly degenerate excitons in Term 2. This expectation is confirmed numerically for bulk CdS in Fig. S4.

Moving on to 2D materials, we expect more significant electron-hole interactions. We investigate the low-energy shift current spectrum in monolayer MoS₂. Fig. 2(a-b) shows our computed absorbance, where a reasonable agreement with experiment is obtained in Fig. 2(b). Fig. 2(c-d) (also Fig. S5) show that the shift current conductivity is significantly enhanced by excitonic interactions. This significant enhancement can be explained by the

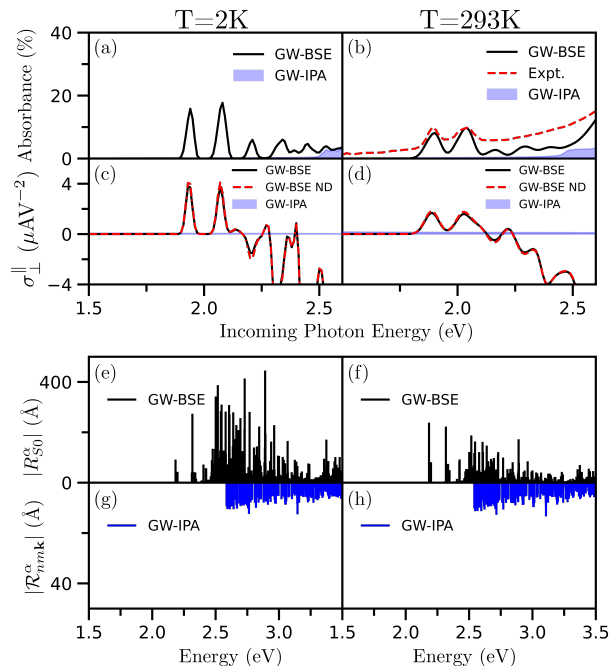


FIG. 2. Optical absorbance spectra (a-b), shift current conductivities (c-d) and shift-vectors computed with GW-BSE and GW-IPA for monolayer MoS₂. \parallel and \perp refer to the armchair and zig-zag directions. The absorbance spectrum is compared with available experimental data [34] in (b). GW-BSE ND in (c-d) refers to the shift current conductivities computed using only Term 2 in Eq. 1 with contributions from excitons that differ in energy by 0.5 eV or less. The GW-IPA shift current conductivities are so small that they are not visible on this plot (see Fig. S5 for a different scale). Exciton-phonon and electron-phonon self-energies, computed at 2K (left panel) and 293 K (right panel), are included in all the BSE and IPA calculations, respectively. The energies on the horizontal axis are $\hbar\Omega_S$ in (e-f) and $\hbar(\omega_n - \omega_m)$ in (g-h).

enhancement in the magnitude of the shift vectors. Fig. 2(e-h) plots the GW-BSE and GW-IPA shift vectors. We see that the magnitudes of the many-body shift vectors are generally one to two orders of magnitude larger than those of the IPA shift vectors. The oscillator strengths are also important for the shift current conductivity (see Eq. 4), and in particular the two lowest energy peaks in the shift current conductivity arise due to the comparatively large oscillator strengths of these A and B excitons, whose shift vector magnitudes are small on the scale of the plots in Fig. 2(e-f).

We next discuss the effects of temperature through the changes in the exciton-phonon self-energies. At higher temperatures, both the imaginary and real parts of the exciton self-energies Ξ_S are larger (see also Fig. S6). The larger imaginary parts of the phonon energies at higher temperatures lead to broader peaks with lower peak heights for both the absorbance and the shift current conductivity (Fig. 2(a-d)). In general, the magnitudes of the many-body shift vectors decrease with tem-

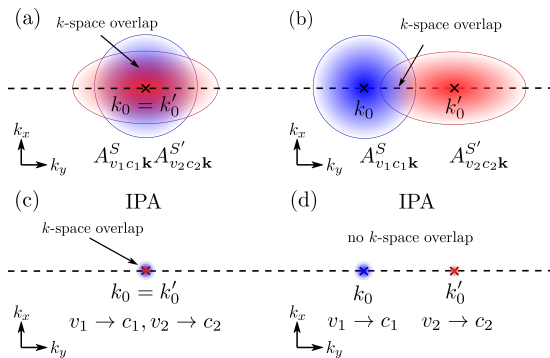


FIG. 3. Schematic illustrating the origin of excitonic enhancement of the many-body shift vector. (a-b) Two excitons with Gaussian envelope functions centered at (a) the same k -point, (b) different k -points. (c-d) The excitons in (a) and (b), respectively, in the IPA limit, where the Gaussian envelope functions collapse to delta functions at k_0 and k'_0 .

perature. This temperature dependence can be understood mathematically through Eq. 2, where the sum of the imaginary part of the self-energies for S and S' appears in the denominator for $r_{S',S}^\alpha$ (see S5) [24]. Recalling that the many-body shift vector as a positional shift in charge centers, we can also rationalize the temperature dependence of the shift vector from the general expectation that excitons are more strongly scattered by phonons in real space at higher temperatures, hindering the charge shift when excited from the ground state. The temperature dependence of the IPA shift vectors (Fig. 2(g-h)) and the IPA shift current conductivity (Fig. S5) is less evident than for the many-body case in this energy range. One reason for this observation is that the exciton self-energies are larger than the quasiparticle self-energies (see also Fig. S7).

We now discuss why large electron-hole interactions in 2D materials lead to a significant enhancement of the magnitudes of the shift current conductivity and shift vector, which we observe in general across the range of incoming photon energies. This excitonic enhancement has also been observed for other non-linear optical responses [21, 22, 26] and is in contrast to the case of the linear optical response, where excitonic effects lead to sharper peaks at some energies, but the oscillator strengths are governed by a sum rule [23]. The origin of this overall excitonic enhancement for the nonlinear optical response is the interexciton dipole transition matrix elements, which we see in Eq. 1 and in the general non-linear optical response [26]. In particular, the expressions for $r_{S',S}^\alpha$ and $p_{S',S}^\beta$ (Eqs. 7 and 8), with $S \neq S'$ are non-zero only when the excitons S and S' overlap in k -space.

Fig. 3(a-b) shows excitons with Gaussian envelope functions centered at the same (a) and different (b) k -points, overlapping in k -space. Noting that the many-body shift current reduces to the IPA expression in the

IPA limit, we can use the lens of the many-body formalism to provide new insights into the IPA shift current. In the IPA, the excitons collapse to a single k -point, corresponding to momentum-direct optical transitions between Bloch states (Fig. 3(c-d)). Thus, most of the exciton pairs contributing in the many-body picture due to k -space overlap would not contribute in the IPA (Fig. 3(d)), explaining why the IPA shift current is typically an order of magnitude smaller than the BSE shift current. This physical picture can also be applied directly to explain the excitonic enhancement of the shift vector, using Eq. 2. The stronger the electron-hole interactions, the more tightly bound the excitons are in real space, and thus, the more spread out the excitons are in k -space, and the more likely pairs of excitons can overlap in k -space. As such, we expect that stronger excitonic interactions lead to more significant excitonic enhancements of the non-linear optical response.

In Fig. 4, we illustrate first principles results for $|r_{S',S}^\alpha|$ and the k -space overlap between excitons, contributing to the many-body shift vector for one of the excitons in MoS₂. We comment that $|r_{S',S}^\alpha|$ drops off quickly as $\Omega_{S'}$ increases, enabling numerical convergence when applying the sum rule. Fig. 4(b-c) shows the k -space overlap between excitons $S' = 1$ and $S = 3$.

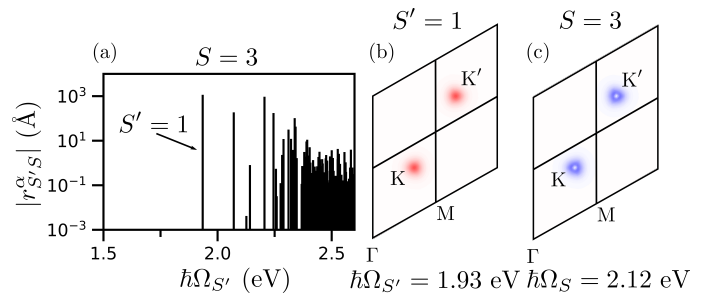


FIG. 4. Many-body shift vector analysis for exciton $S = 3$ in monolayer MoS₂. (a) Plot of $|r_{S',S}^\alpha|$ for $S = 3$ as a function of the energy of exciton S' . The largest contribution comes from the coupling to $S' = 1$. (b-c) Distribution of the exciton wavefunction $|A_{vc\mathbf{k}}^S|$ in reciprocal space for (b) $S' = 1$ and (c) $S = 3$. Both wavefunctions are spread around the K and K' points.

In conclusion, we have discussed the origin of the shift current in the many-body picture, presenting two equivalent but complementary interpretations. One interpretation is that the many-body shift current arises from positional shifts of charge centers from the ground state to the many-body excited states, weighted by the square of the optical transition matrix elements for the excitons. It is helpful to comment here that the shift current is defined as an expectation value of velocity, and unlike a ballistic current, does not require free carriers [35]. An alternative interpretation of the origin of the shift current, related to the first through a many-body sum rule, describes the many-body shift

current as being dominated by processes involving transitions from $|0\rangle$ to $|S'\rangle$, $|S'\rangle$ to $|S\rangle$ and $|S\rangle$ to $|0\rangle$, especially when S is nearly degenerate with S' (see Fig. S8). This second interpretation allows us to explain the origin of excitonic enhancement of non-linear optical processes. In particular, we predict that shift currents can be enhanced by choosing inversion-symmetry breaking layered 2D systems with strong electron-hole interactions, and a high density of nearly-degenerate excitons optically active in the solar spectrum. Using the Computational 2D Materials Database [24, 36], we list in the SI other 2D materials which lack inversion symmetry and have a suitable band gap, that may be promising for bulk photovoltaics.

Note added. A theoretical paper describing the many-body shift current from a geometrical perspective was uploaded to arXiv [27] after the first submission of this manuscript.

ACKNOWLEDGEMENTS

This work is supported by NUS and the National Research Foundation (NRF), Singapore, under the NRF medium-sized centre programme. Calculations were performed on the computational cluster in the Centre for Advanced 2D Materials and the National Supercomputing Centre, Singapore. ML also thanks LQN Cheng and YL Kwok for support and discussions.

* phyqsy@nus.edu.sg

- [1] J. E. Spanier, V. M. Fridkin, A. M. Rappe, A. R. Akbashev, A. Polemi, Y. Qi, Z. Gu, S. M. Young, C. J. Hawley, D. Imbrenda, *et al.*, *Nat. Photonics* **10**, 611 (2016).
- [2] J. Sipe and A. Shkrebtii, *Phys. Rev. B* **61**, 5337 (2000).
- [3] B. I. Sturman, *Physics-Uspokhi* **63**, 407 (2020).
- [4] V. Belinicher, E. Ivchenko, and B. Sturman, *Zh. Eksp. Teor. Fiz* **83**, 649 (1982).
- [5] W. Kraut and R. von Baltz, *Phys. Rev. B* **19**, 1548 (1979).
- [6] C. Aversa and J. Sipe, *Phys. Rev. B* **52**, 14636 (1995).
- [7] S. M. Young and A. M. Rappe, *Phys. Rev. Lett.* **109**, 116601 (2012).
- [8] A. M. Cook, B. M. Fregoso, F. De Juan, S. Coh, and J. E. Moore, *Nat. Commun.* **8**, 1 (2017).
- [9] M. Rohlfing and S. G. Louie, *Phys. Rev. B* **62**, 4927 (2000).
- [10] Y. Jia, M. Zhao, G. Gou, X. C. Zeng, and J. Li, *Nanoscale Horiz.* **4**, 1113 (2019).
- [11] C. Wang, L. You, D. Cobden, and J. Wang, *Nat. Mater.*, **1** (2023).
- [12] Y. Li, J. Fu, X. Mao, C. Chen, H. Liu, M. Gong, and H. Zeng, *Nat. Commun.* **12**, 5896 (2021).
- [13] I. Abdelwahab, B. Tilmann, Y. Wu, D. Giovanni, I. Verzhbitskiy, M. Zhu, R. Berté, F. Xuan, L. d. S. Menezes, G. Eda, *et al.*, *Nat. Photonics* **16**, 644 (2022).
- [14] I. Abdelwahab, B. Tilmann, X. Zhao, I. Verzhbitskiy, R. Berté, G. Eda, W. L. Wilson, G. Grinblat, L. de S. Menezes, K. P. Loh, *et al.*, *Adv. Opt. Mater.*, **2202833** (2023).
- [15] Q. Guo, X.-Z. Qi, L. Zhang, M. Gao, S. Hu, W. Zhou, W. Zang, X. Zhao, J. Wang, B. Yan, *et al.*, *Nature* **613**, 53 (2023).
- [16] Z. Qin, Y. Chen, K. Zhu, and Y. Zhao, *ACS Mater. Lett.* **3**, 1402 (2021).
- [17] U. K. Aryal, M. Ahmadpour, V. Turkovic, H.-G. Rubahn, A. Di Carlo, and M. Madsen, *Nano Energy* **94**, 106833 (2022).
- [18] J. Wu, H. Ma, P. Yin, Y. Ge, Y. Zhang, L. Li, H. Zhang, and H. Lin, *Small Science* **1**, 2000053 (2021).
- [19] Z. Tang, S. Chen, D. Li, X. Wang, and A. Pan, *J. Materiomics* **9**, 551 (2023).
- [20] G. Wang, A. Chernikov, M. M. Glazov, T. F. Heinz, X. Marie, T. Amand, and B. Urbaszek, *Rev. Mod. Phys.* **90**, 021001 (2018).
- [21] Y.-H. Chan, D. Y. Qiu, F. H. da Jornada, and S. G. Louie, *PNAS* **118**, e1906938118 (2021).
- [22] Y.-S. Huang, Y.-H. Chan, and G.-Y. Guo, *Phys. Rev. B* **108**, 075413 (2023).
- [23] F. Bassani, in *Encyclopedia of Condensed Matter Physics*, edited by F. Bassani, G. L. Liedl, and P. Wyder (Elsevier, Oxford, 2005) pp. 200–206.
- [24] See Supplemental Material at [url], which includes Refs. [6,9,13,26,29,34], for computational details, derivation of equations and supporting figures.
- [25] J. Ahn, G.-Y. Guo, and N. Nagaosa, *Phys. Rev. X* **10**, 041041 (2020).
- [26] F. Xuan, M. Lai, Y. Wu, and S. Y. Quek, *Phys. Rev. Lett.* **132**, 246902 (2024).
- [27] R. Resta, *arXiv* 2402.12489 (2024).
- [28] L. X. Benedict, E. L. Shirley, and R. B. Bohn, *Phys. Rev. Lett.* **80**, 4514 (1998).
- [29] M. S. Hybertsen and S. G. Louie, *Phys. Rev. B* **34**, 5390 (1986).
- [30] E. Blount, in *Solid state physics*, Vol. 13 (Elsevier, 1962) pp. 305–373.
- [31] G. Antonius and S. G. Louie, *Phys. Rev. B* **105**, 085111 (2022).
- [32] F. Giustino, M. L. Cohen, and S. G. Louie, *Phys. Rev. B* **76**, 165108 (2007).
- [33] M. Sotome, M. Nakamura, T. Morimoto, Y. Zhang, G.-Y. Guo, M. Kawasaki, N. Nagaosa, Y. Tokura, and N. Ogawa, *Phys. Rev. B* **103**, L241111 (2021).
- [34] K. F. Mak, C. Lee, J. Hone, J. Shan, and T. F. Heinz, *Phys. Rev. Lett.* **105**, 136805 (2010).
- [35] A. M. Burger, R. Agarwal, A. Aprelev, E. Schrubba, A. Gutierrez-Perez, V. M. Fridkin, and J. E. Spanier, *Sci. Adv.* **5**, eaau5588 (2019).
- [36] S. Hastrup, M. Strange, M. Pandey, T. Deilmann, P. S. Schmidt, N. F. Hinsche, M. N. Gjerding, D. Torelli, P. M. Larsen, A. C. Riis-Jensen, *et al.*, *2D Mater.* **5**, 042002 (2018).